Neuron
Article

Transsynaptic Progression of Amyloid-β-Induced Neuronal Dysfunction within the Entorhinal-Hippocampal Network

Julie A. Harris,[1,2] Nino Devidze,[1] Laure Verret,[1,2] Kaitlyn Ho,[1] Brian Halabisky,[1,2] Myo T. Thwin,[1] Daniel Kim,[1] Patricia Hamto,[1] Iris Lo,[1] Gui-Qiu Yu,[1] Jorge J. Palop,[1,2] Eliezer Masliah,[3,4] and Lennart Mucke[1,2,*]
[1]Gladstone Institute of Neurological Disease, San Francisco, CA 94158, USA
[2]Department of Neurology, University of California, San Francisco, San Francisco, CA 94158, USA
[3]Department of Neurosciences
[4]Department of Pathology
University of California, San Diego, La Jolla, CA 92093, USA
*Correspondence: lmucke@gladstone.ucsf.edu
DOI 10.1016/j.neuron.2010.10.020

SUMMARY

The entorhinal cortex (EC) is one of the earliest affected, most vulnerable brain regions in Alzheimer's disease (AD), which is associated with amyloid-β (Aβ) accumulation in many brain areas. Selective overexpression of mutant amyloid precursor protein (APP) predominantly in layer II/III neurons of the EC caused cognitive and behavioral abnormalities characteristic of mouse models with widespread neuronal APP overexpression, including hyperactivity, disinhibition, and spatial learning and memory deficits. APP/Aβ overexpression in the EC elicited abnormalities in synaptic functions and activity-related molecules in the dentate gyrus and CA1 and epileptiform activity in parietal cortex. Soluble Aβ was observed in the dentate gyrus, and Aβ deposits in the hippocampus were localized to perforant pathway terminal fields. Thus, APP/Aβ expression in EC neurons causes transsynaptic deficits that could initiate the cortical-hippocampal network dysfunction in mouse models and human patients with AD.

INTRODUCTION

Alzheimer's disease (AD) is characterized by progressive memory impairments (Blennow et al., 2006). Since encoding of various forms of memory requires an intact entorhinal-hippocampal circuit (Eichenbaum and Lipton, 2008; Squire et al., 2004), it is not surprising that this network is severely affected by AD. Neurons in superficial layers of the entorhinal cortex (EC) form synapses via the perforant pathway in all hippocampal subregions, including the dentate gyrus (DG), CA3, CA1, and subiculum, with the largest projection to the granule cells (GCs) of the DG (van Groen et al., 2003; van Strien et al., 2009). In mice, DG GCs receive afferent input primarily from layer II neurons of the EC; projections to CA3 and CA1 originate mostly from layer III (van Groen et al., 2003; van Strien et al., 2009). Synaptic connections between mossy fibers of DG GCs and CA3 neurons and Schaffer collaterals from CA3 to CA1 neurons complete the forward hippocampal polysynaptic circuit.

In the entorhinal-hippocampal network, the EC is a particularly early target in AD. Significant loss of neurons in EC layer II occurs in the beginning stages of AD (Gómez-Isla et al., 1996). Neurofibrillary tangles (NFTs), a hallmark of AD, are seen primarily in the EC in mild AD and "spread" to the hippocampus and other cortical areas as the disease progresses (Braak and Braak, 1991). Structural and functional imaging studies also show early, selective atrophy and hypometabolism in the EC of patients with mild cognitive impairment or early-stage AD (Masdeu et al., 2005; Wu and Small, 2006).

Amyloid-β (Aβ) peptides generated from amyloid precursor protein (APP) by proteolytic cleavage likely play a causal role in AD pathogenesis (Tanzi and Bertram, 2005; Walsh and Selkoe, 2004). Although the precise mechanisms of Aβ toxicity are unclear, oligomeric forms of Aβ may contribute to cognitive decline by altering synaptic structure and function (Palop and Mucke, 2010; Selkoe, 2008; Shankar et al., 2008). Transgenic mouse models that overexpress mutant APP and produce high levels of Aβ show amyloid plaque deposition, synaptic deficits, learning and memory impairments, and other behavioral abnormalities (Games et al., 1995; Götz et al., 2004; Hsia et al., 1999; Hsiao et al., 1996; Kobayashi and Chen, 2005). Pathogenic Aβ assemblies elicit aberrant excitatory activity in cortical-hippocampal networks and compensatory responses that are particularly evident in the DG (Palop et al., 2003, 2007).

It is unclear which brain regions or cell types are first affected by APP/Aβ to ultimately elicit network dysfunction. AD may spread through anatomically and functionally connected brain regions (Braak and Braak, 1991; Braak et al., 2006; Buckner et al., 2005), perhaps by a prion-like mechanism (Eisele et al., 2009; Frost and Diamond, 2010). In AD patients, the EC is an early target and could be the region from which AD invades other brain regions. Neuronal alterations starting in the EC could propagate throughout EC-hippocampal-cortical networks. It has been hypothesized that AD originates in the EC because APP expression was higher in EC layer II neurons than in other

cortical areas in cognitively intact people (Roberts et al., 1993); levels further increased in early-stage AD but declined in late stages. However, more recent studies have not found higher APP levels in EC neurons of cognitively intact individuals or differences in expression in patients with mild to late-stage AD (Liang et al., 2007, 2008).

Given its various effects on synaptic function (Palop and Mucke, 2010), Aβ could be the key mediator of the proposed transsynaptic (i.e., across a synapse) progression of AD. In this study, we determined whether production of human Aβ by EC neurons can elicit AD-like behavioral deficits and cortical-hippocampal network dysfunction by using mice with transgene-derived APP expression primarily in neurons of the superficial layers of the EC and the pre/parasubiculum. These mice exhibited disinhibition, hyperactivity, and age-related cognitive deficits in spatial learning and memory tasks. Similar behavioral phenotypes have been described in transgenic mice with widespread neuronal expression of APP/Aβ (Cheng et al., 2007; Chin et al., 2005; Götz et al., 2004; Kobayashi and Chen, 2005; Palop et al., 2003). Soluble Aβ levels were high in the DG of young mice with APP/Aβ expression in EC neurons, suggesting presynaptic synthesis and/or release of Aβ. Aβ deposits in the hippocampus of older mice were mostly seen in perforant pathway terminal fields. Finally, selective overexpression of APP/Aβ in EC neurons also increased cortical network excitability, synaptic loss in the outer molecular layer of the DG, and alterations in synaptic-activity-related molecules in GCs of the DG that typically reflect such aberrant network activity.

RESULTS

Expression of APP in the EC of Neuropsin-tTA/Tet-APP Doubly Transgenic Mice

To produce mice with regionally selective overexpression of APP with familial AD mutations, we bred neuropsin-tTA (Yasuda and Mayford, 2006) and tet-APP mice (Jankowsky et al., 2005) (Figure 1A). The tet-APP transgene encodes a chimeric mouse APP with a humanized Aβ domain. Mice were not treated with doxycycline, allowing transactivation of tet-APP expression by tTA. Offspring with both transgenes (EC-APP mice) expressed mutant APP primarily in the parahippocampal cortex, including the medial EC and pre/parasubiculum (Figures 1B–1D). This pattern is in stark contrast to the spatially generalized expression pattern of APP in other APP transgenic lines, such as the human APP (hAPP) transgenic line J20 (Figures S1A and S1B), and similar to that of other tet-regulatable transgenes after crosses with the neuropsin-tTA line (Yasuda and Mayford, 2006). However, we observed some transgene expression in the lateral EC and scattered cells with faint expression in superficial layers of other cortical regions and area CA of the hippocampus (Figures 1B–1D and S2). No mutant APP was detected in NTG or singly tTA transgenic mice, and only very low levels of mutant APP were detected in the CA region of tet-APP singly transgenic mice, suggesting minimal "leakiness" of transgene expression in the absence of tTA (Figures S3A and S3B). Cells expressing mutant APP in the EC were mostly layer II or III neurons (Figure 1D, middle). No mutant APP was detected in GCs of the DG, although some scattered APP-positive cells were seen in the hilus (Figure 1D, right).

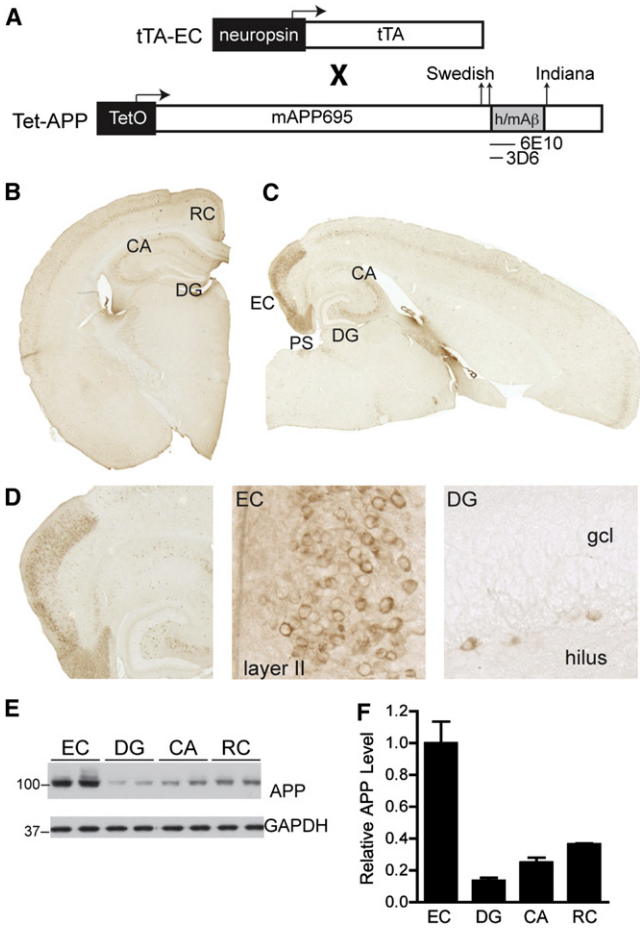

Figure 1. Restricted Cortical Expression of Mutant APP in EC-APP Mice

(A) Transgenes used to generate tTA-EC and tet-APP mouse lines. When crossed, mice carrying both transgenes expressed mutant APP primarily in the EC.

(B and C) Representative images of coronal (B) and horizontal (C) brain sections from EC-APP mice stained for chimeric human/mouse APP (h/mAPP) with anti-human Aβ antibody 6E10. Prominent APP expression was observed in medial EC and in pre- and parasubiculum (PS). Hippocampal APP labeling was faint in scattered cells of CA regions.

(D) Higher magnification images of EC and DG in an EC-APP mouse show neuronal expression of APP predominantly in superficial layers of the EC. No transgene expression was observed in the granular cell layer (gcl) of the DG; scattered APP-positive cells were seen in the hilus.

(E and F) Relative APP levels in different brain regions of EC-APP mice were determined by western blotting (E) and quantified by densitometry (F). GAPDH served as a loading control. EC had the highest APP levels, followed by RC, where APP levels were less than 40% of those in EC. Values are mean ± SEM.

Measurement of mutant APP levels in microdissected brain regions by western blotting confirmed the immunohistochemical analyses. The EC had the highest level of full-length mutant APP; levels in the DG (13%) and CA (25%) (Figures 1E and 1F) were lower and similar to the "leaky" expression detected in tet-APP singly transgenic mice (Figure S3). The

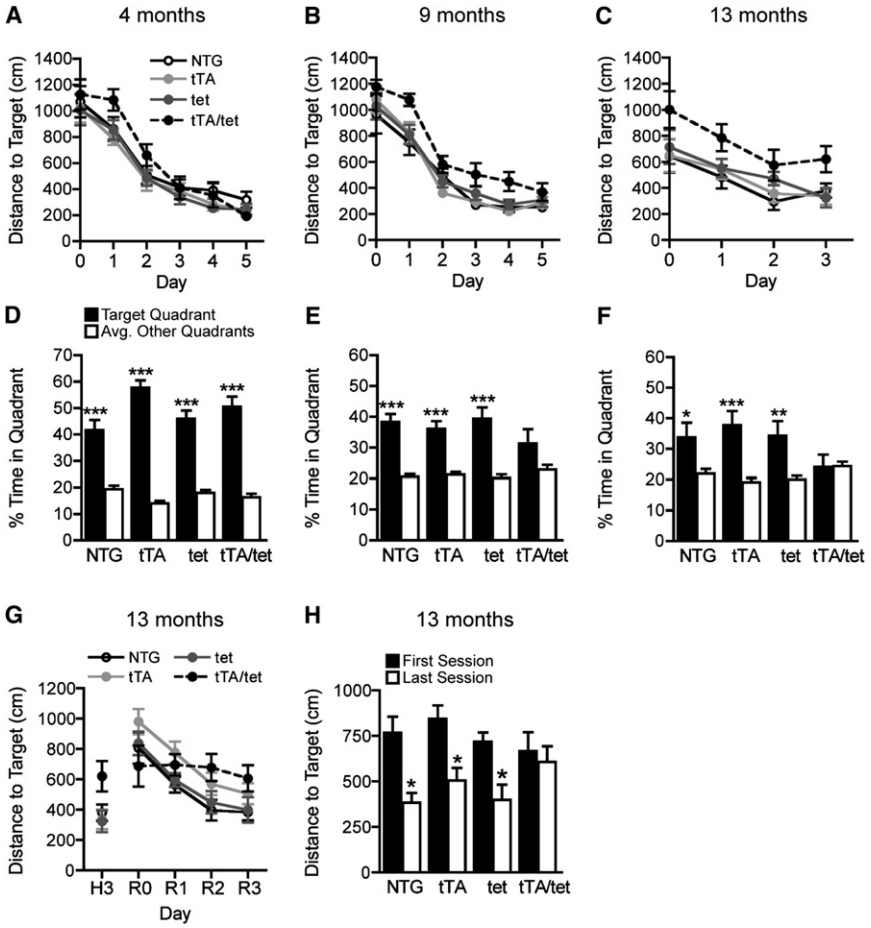

Figure 2. EC-APP Mice Have Age-Dependent Deficits in Spatial Learning and Memory

(A–C) At 4 (A), 9 (B), and 13 (C) months of age, mice of the four genotypes were trained for 3–5 days to locate a hidden platform in the MWM. By 9 months, EC-APP (tTA/tet) mice showed impaired learning relative to the other groups ($p < 0.001$ for genotype, repeated-measures ANOVA). Their learning deficits persisted at 13 months ($p < 0.01$ for genotype, repeated-measures ANOVA).

(D–F) At each age, probe trials were conducted 24 hr after the last training session. At 4 months, all groups showed a clear preference for the target quadrant. At 9 months, only EC-APP mice failed to spend significantly more time in the target quadrant than in the other quadrants. At 13 months, EC-APP mice spent comparable proportions of time in target and nontarget quadrants, whereas the other groups still favored the target quadrant.

(G–H) Thirteen-month-old EC-APP mice have deficits in a spatial reversal-learning task. After the probe trial (F), the platform location was changed, and mice were trained for 3 more days to the new location (reversal phase). In contrast to the controls, EC-APP mice did not improve their performance during this reversal task (G) ($p < 0.0005$ for effect of training day, repeated-measures ANOVA in the control groups only). Distances to the new target location were shorter in the last than the first training sessions in the controls, but not in EC-APP mice (H). *$p < 0.05$, **$p < 0.005$, ***$p < 0.0005$ versus the average percent time spent in nontarget quadrants by t test (D–F) or versus the first session by t test (H); n = 10–13 mice/group. Values are mean ± SEM.

retrosplenial/posterior cingulate cortex (RC), which also showed some immunostaining for mutant APP (Figure 1B), had ~36% of the expression levels in the EC (Figure 1F).

In situ hybridization with an oligonucleotide probe that specifically recognizes APP mRNA encoding the human Aβ domain confirmed that the pattern of transgene-derived APP mRNA expression matched the immunostaining pattern obtained with the anti-human Aβ antibody 6E10 (Figure S4). Transgene expression in the EC was higher in EC-APP mice than in hAPP-J20 mice, whose transgene expression levels were highest in the DG (Figures S1C, S1D, and S4C).

Expression of Mutant APP Predominantly in the EC Impairs Spatial Learning and Memory

Spatial learning and memory were tested in the Morris water maze (MWM). At different ages, mice were trained over 5 consecutive days to navigate to a hidden platform using spatial cues outside the maze. At 4 months, EC-APP (tTA/tet) mice and controls (NTG, tTA, and tet-APP) did not differ in their ability to learn this task, as reflected in the total distance covered (Figure 2A) to reach the target platform. EC-APP mice displayed a trend toward delayed acquisition in the first 2 days of training at 4 months and at 9 months were significantly impaired relative to all control groups (Figure 2B). Mice were trained in the water maze once more at 13 months of age for 3 days; EC-APP mice continued to have spatial learning deficits (Figure 2C). Latency to reach the target platform revealed similar differences among groups (data not shown). Swim speeds during hidden platform training were not different among the groups of mice, and all groups performed equally well in the cued version of the task (data not shown).

The target platform was removed 24 hr after the last day of hidden training to assess memory retention at each age. At 4 months, all groups spent more time searching in the target quadrant (where the platform had been located) than in the other quadrants, indicating good memory retention (Figure 2D). At 9 months, all control groups, but not EC-APP mice, showed a significant preference for the target quadrant (Figure 2E). By 13 months, the control groups still favored the target quadrant, whereas EC-APP mice showed no preference for the target quadrant, indicating very poor spatial memory (Figure 2F).

Next, we analyzed spatial reversal learning in 13-month-old mice. For this test, the target platform was moved to a new location 24 hr after the probe trial that followed the initial hidden platform training. Mice were trained to find this new location for 3 consecutive days. Over time, all control groups, but not EC-APP mice, showed significant improvements (Figure 2G). EC-APP mice were the only group that did not swim shorter distances

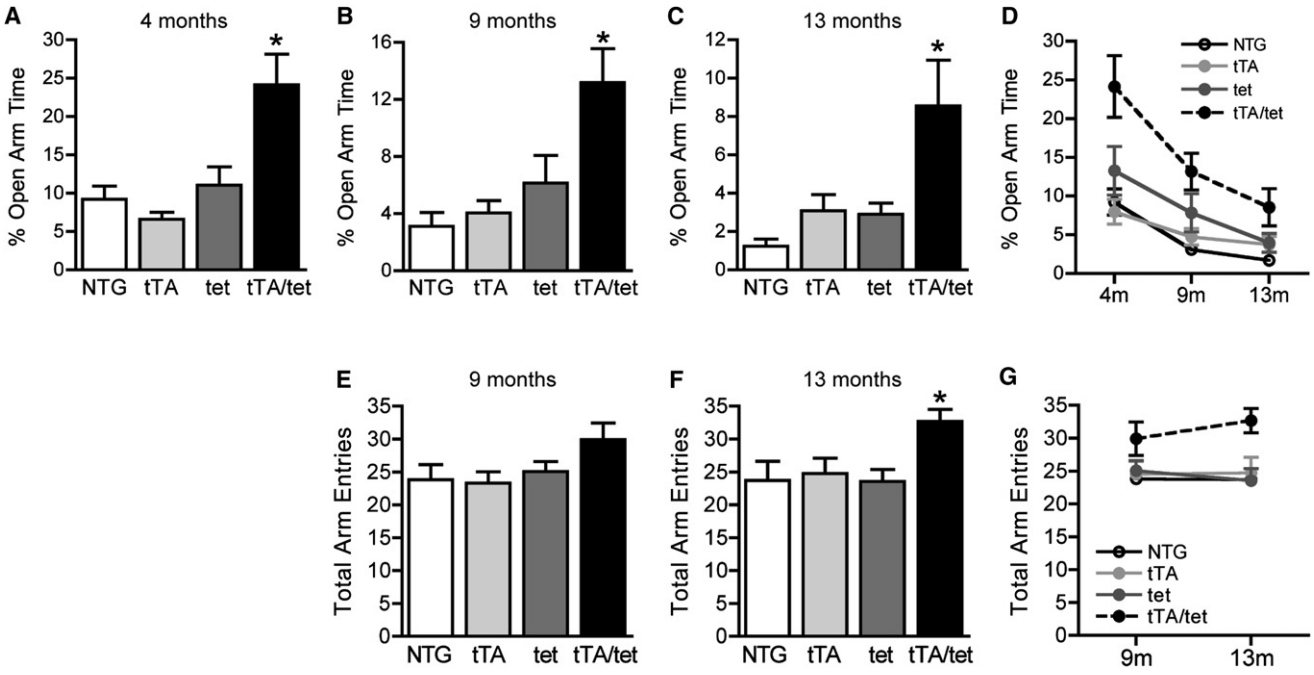

Figure 3. EC-APP Mice Show Abnormal Phenotypes in the Elevated Plus Maze and Y-Maze

(A–C) Percent time spent in open arms of an elevated plus maze was recorded over 5 min. At all ages, EC-APP (tTA/tet) mice spent more time in open arms than control groups. *$p < 0.05$ versus all other groups by ANOVA and Tukey test.

(D) All groups spent less time in open arms during subsequent tests. $p < 0.0001$ for effects of genotype and age, two-way ANOVA.

(E–G) EC-APP mice are hyperactive in the Y-maze. Total arm entries were monitored over 6 min at 9 (E) and 13 (F) months. Compared with controls, EC-APP (tTA/tet) mice showed a trend toward increased activity at 9 months and clear hyperactivity at 13 months. *$p < 0.05$ versus all other groups, ANOVA and Newman-Keuls post hoc test. None of the groups showed habituation in Y-maze activity during the second exposure (G). $p < 0.05$ for genotype only, two-way ANOVA. n = 10–13 mice/group. Values are mean ± SEM.

in the last session than in the first (Figure 2H). The learning and retention deficits in the initial component of water maze testing (Figures 2C and 2F) complicate the interpretation of this reversal-learning deficit. However, the downward slope of their first learning curves suggests that EC-APP mice learned this task initially, albeit less well than the control groups (Figure 2C, $p = 0.06$, ANOVA effect of time) but could not learn in the reversal paradigm.

Expression of Mutant APP Predominantly in the EC Causes Additional Behavioral Abnormalities

Decreased time spent in the open arms of an elevated plus maze is a measure of increased anxiety (Belzung and Griebel, 2001). Several lines of hAPP transgenic mice spend more time in the open arms than NTG controls, suggesting lower levels of anxiety or disinhibition (Cheng et al., 2007; Chin et al., 2005; Harris et al., 2010; Ognibene et al., 2005). EC-APP mice also spent significantly more time in the open arms than the control groups at all ages (Figures 3A–3C). All groups showed some habituation to the elevated plus maze with repeated testing (Figure 3D).

Different lines of hAPP transgenic mice also show hyperactivity in several arenas, including the open field and Y-maze (Chin et al., 2005; Kobayashi and Chen, 2005; Roberson et al., 2007). At 9 months, EC-APP mice showed a trend toward increased total activity in the Y-maze (Figure 3E) and by 13 months were clearly hyperactive compared to controls (Figure 3F). There was no habituation to repeated Y-maze testing in any group (Figure 3G). EC-APP mice were not impaired in the working memory component of the Y-maze (data not shown). Unlike transgenic lines with widespread hAPP expression, EC-APP mice showed no alterations in locomotor activity in the open field at any age (Figure S5).

Expression of Mutant APP Predominantly in the EC Elicits Alterations in Calcium- and Synaptic Activity-Related Proteins in the DG

Previously, we identified strong correlations between learning and memory deficits and depletions of calbindin-D_{28K} and Fos in GCs of the DG in hAPP-J20 mice (Palop et al., 2003). In addition, DG GCs of hAPP-J20 mice ectopically expressed neuropeptide Y (NPY) in the mossy fiber pathway to CA3 (Palop et al., 2007). NPY levels were also increased in the DG molecular layer, likely a result of enhanced expression by interneurons (Palop et al., 2007). Most of these DG-specific molecular alterations are probably compensatory responses to Aβ-induced aberrant network activity (Palop et al., 2007).

To determine whether alterations in these proteins are caused by APP/Aβ expression in the EC, we measured their levels in the DG of two groups of EC-APP mice (Figure 4): 6-month-old naive mice that had never been tested behaviorally and mice that were tested at 4, 9, and 13 months. Although EC-APP mice had no transgene-derived APP in DG GCs (Figure 1), they had lower

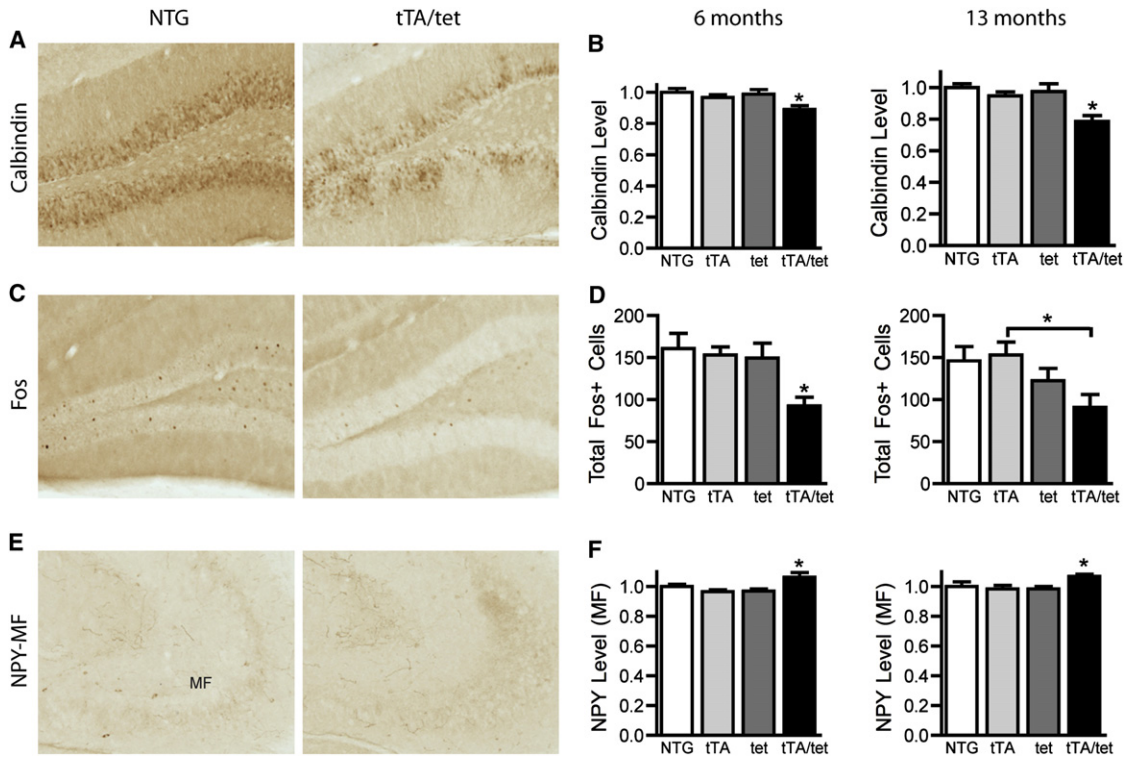

Figure 4. EC-APP Mice Have Abnormalities in Synaptic Activity-Related Proteins in the DG

(A–F) Representative coronal sections of the DG from 6-month-old NTG and EC-APP (tTA/tet) mice (A, C, and E) and quantitative results from 6- and 13-month-old mice (B, D, and F). Brain sections from mice of all four genotypes were immunostained for calbindin, Fos, or NPY and quantified by densitometry or cell counts. ANOVA revealed a significant effect of genotype on all protein measures. *$p < 0.05$ versus all other groups or as indicated by brackets with Newman-Keuls post hoc test. n = 14–15 mice/group (6 months) or n = 6–9 mice/group (13 months). Values are mean ± SEM.

calbindin levels in the molecular layer at 6 and 13 months than age-matched controls (Figures 4A and 4B), fewer GCs expressing Fos at both ages (Figures 4C and 4D), and a subtle but significant increase in NPY expression in mossy fibers (Figures 4E and 4F). NPY expression in the molecular layer of the DG was unchanged (data not shown), suggesting that expression of APP/Aβ in the EC and perforant pathway selectively affects GCs but not interneurons in the DG.

Expression of Mutant APP Predominantly in the EC Induces Abnormal Network Excitability

EEG recordings in other lines of APP transgenic mice revealed cortical and hippocampal epileptic activity (Minkeviciene et al., 2009; Palop et al., 2007). Since EC-APP mice displayed several molecular changes in the DG that indicate such network alterations (Figure 4) (Palop et al., 2003, 2007), we hypothesized that they would also have periods of aberrant excitatory neuronal activity. To test this hypothesis, we used video and EEG recordings to monitor EC-APP and control groups of mice at 4–5 months of age over 24 hr. Bilateral recording electrodes over the parietal cortex (PC) revealed very few or no sharp wave discharges (SWDs) in control mice (Figures 5A–5C and 5F) and an average of 30 SWDs per hour in EC-APP mice (Figures 5D–5F). No seizures occurred. Thus, EC-APP mice have widespread cortical network alterations, even though mutant APP expression is restricted primarily to the EC. After the recordings, we confirmed that the mice had no Aβ deposition in the PC (data not shown).

Synaptic Deficits in EC-APP Mice

Loss of synaptophysin-immunoreactive presynaptic terminals in specific brain regions is characteristic of AD pathology and correlates well with the degree of cognitive impairments (Sze et al., 1997; Terry et al., 1991). Several hAPP lines, including J20, show similar synaptic alterations (Chin et al., 2004; Galvan et al., 2006; Hsia et al., 1999; Mucke et al., 2000; Tomiyama et al., 2010). In 6- and 13-month-old EC-APP mice, significant synaptophysin loss was observed in the outer molecular layer of the DG, a terminal field of the perforant path (Figures 6A and 6B). Compared with NTG mice, EC-APP mice also showed a loss of synaptophysin in the stratum radiatum of CA1, where the Schaffer collaterals terminate, but it was subtle and detectable only at 13 months (Figures 6C and 6D). Thus, at older ages, some synaptic loss may occur downstream of the initial impairment of the perforant path to GC synapse.

To determine whether expression of mutant APP in the EC also impairs synaptic functions in the hippocampus, we measured long-term potentiation (LTP) and baseline synaptic transmission at the perforant path to GC synapses and at the Schaffer collateral synapses in CA1. hAPP-J20 mice show distinct

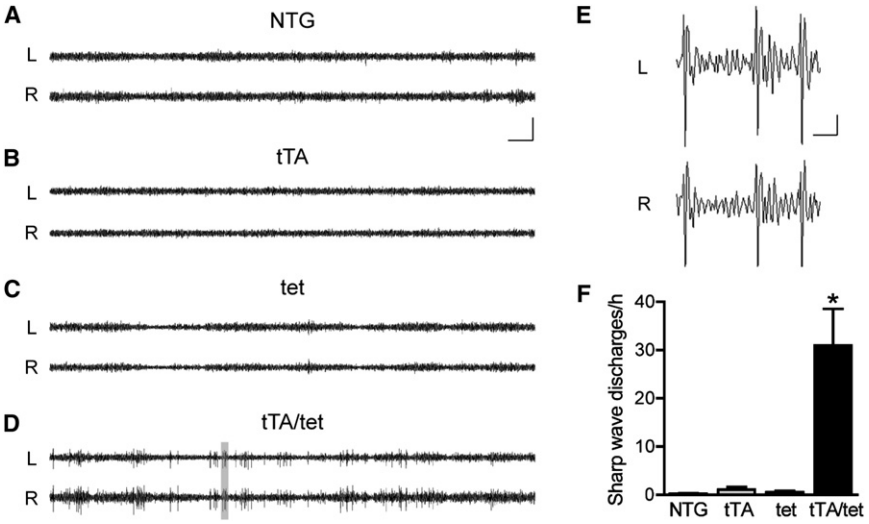

Figure 5. Epileptiform Activity in Parietal Cortex of EC-APP Mice

(A–C) Bilateral EEG recordings were performed in 4- to 5-month-old mice of all four genotypes for 24 hr. Representative traces from controls show normal EEG activity with no or very infrequent sharp wave discharges (SWDs).

(D) In contrast, EC-APP (tTA/tet) mice displayed frequent SWDs.

(E) The gray area in (D) was magnified to reveal waveforms of spike discharges in EC-APP mice.

(F) Quantification of total SWDs per hour revealed a significantly greater frequency of SWDs in EC-APP mice than in all other groups. $p < 0.0005$ for genotype by ANOVA and $^*p < 0.05$ versus all other groups by Tukey post hoc test. n = 4–7 mice/group. L, left PC; R, right PC. Values are mean ± SEM. Scale bars: (A), 10 s and 500 μV; (E), 0.5 s and 100 μV.

electrophysiological abnormalities at different synapses (Palop et al., 2007). Specifically, LTP is impaired and baseline synaptic transmission is normal in the perforant path to GC synapses, whereas baseline synaptic transmission is impaired and LTP is normal in Schaffer collateral synapses onto CA1 pyramidal cells. Recording of extracellular field excitatory postsynaptic potential (fEPSP) revealed no abnormalities in these measures at either synapse in 6-month-old EC-APP mice (data not shown).

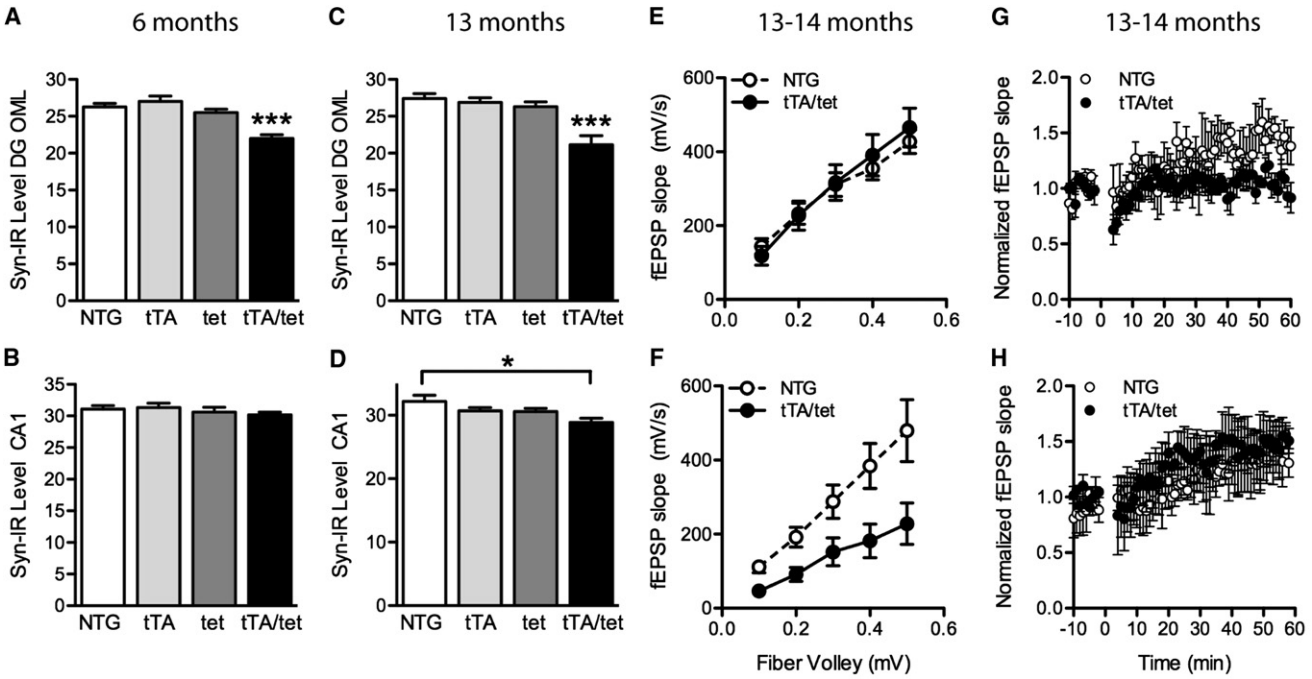

Figure 6. Synaptic Deficits in EC-APP Mice

(A–D) Percent area of sections occupied by synaptophysin-immunoreactive structures in the outer molecular layer of the DG and stratum radiatum of CA1 at 6 (A and B) and 13 (C and D) months of age. At both ages, synaptophysin levels were lower in the DG of EC-APP (tTA/tet) mice than in all control groups (A and C). Genotype affected synaptophysin levels in CA1 at 13 but not 6 months (B and D). n = 6–9 mice/group. $^*p < 0.05$, $^{***}p < 0.0005$ versus all other groups or as indicated by the bracket (Tukey post hoc test).

(E–H) Electrophysiological recordings were obtained in acute hippocampal slices from 13- to 14-month-old EC-APP and NTG mice. The input-output relationship in EC-APP mice was normal at the perforant path-GC synapse in the DG (E, n = 6–7 slices from three mice/genotype), but impaired at the Schaffer collateral-CA1 synapse (F, $p < 0.05$, two-way repeated-measures ANOVA, n = 9–10 slices from 3–5 mice/genotype). LTP was impaired at the perforant path-GC synapse in the DG of EC-APP mice relative to controls (G, $p < 0.05$, repeated-measures ANOVA from 50 to 60 min, n = 3–4 slices from three mice/genotype), but not at the Schaffer collateral-CA1 synapse (H, n = 3–4 slices from 2–3 mice/genotype). All values shown are mean ± SEM.

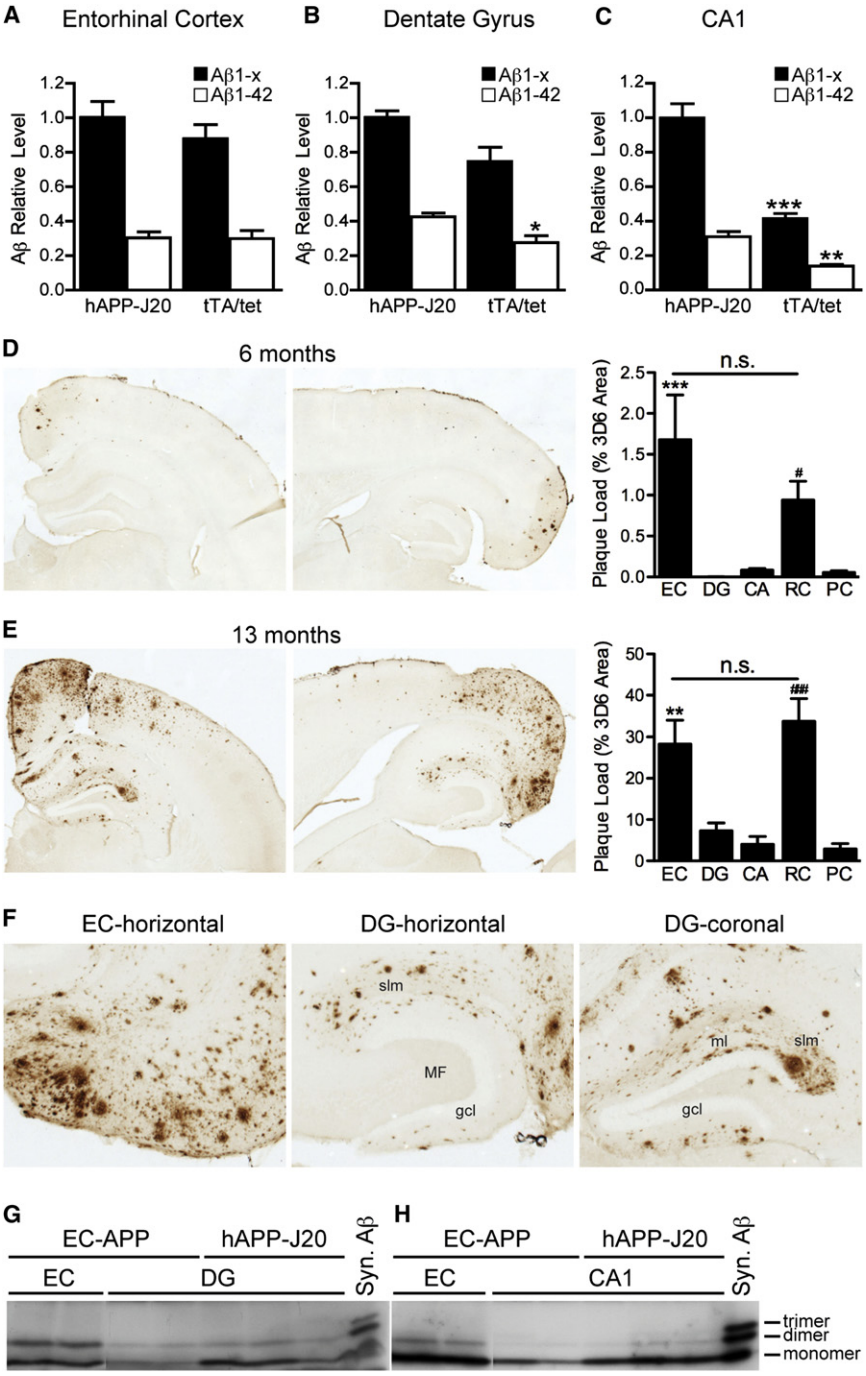

Figure 7. Aβ Levels and Plaque Distribution in Interconnected Brain Regions of Young and Older EC-APP Mice

(A–C) Soluble levels of Aβ1-x and Aβ1-42 were measured before plaque formation in EC (A), DG (B), and CA1 (C) by ELISA in 3-month-old EC-APP (tTA/tet) mice and age-matched hAPP-J20 mice. Levels of Aβ1-x and Aβ1-42 in EC and Aβ1-x in DG were comparable in EC-APP mice and hAPP-J20 mice. Levels of Aβ1-x and Aβ1-42 in CA1 and of Aβ1-42 in DG were lower in EC-APP mice than in hAPP-J20 mice. n = 3–4 mice/genotype. *p < 0.05, **p < 0.005, ***p < 0.0005 versus hAPP-J20 by t test.

(D–F) Immunostaining for Aβ with the 3D6 antibody revealed an age-dependent increase in Aβ deposition in the EC, DG, CA, RC, and PC of EC-APP mice. Representative coronal (left) and horizontal (middle) brain sections for each age are shown in (D) and (E). Percent area covered by 3D6-immunoreactive Aβ deposits was quantified to determine plaque loads. Horizontal sections were used for EC and coronal sections for DG, CA, RC, and PC. Numbers of mice analyzed: at 6 months, n = 15 (coronal; DG, CA, RC, PC) and 9 (horizontal; EC); at 13 months, n = 7 (coronal) and 4 (horizontal). n.s., not significant, **p < 0.005, ***p < 0.0005 EC versus DG, CA, and PC; #p < 0.05, ###p < 0.0005 RC versus DG, CA, and PC by ANOVA and Tukey post hoc test. Values are mean ± SEM. Higher-magnification images from 13-month-old mice showing plaque deposition throughout the EC are shown (F, left). In the DG (F, middle and right), plaques were localized predominantly in the terminal fields of perforant pathway axons from the EC: stratum lacunosum moleculare (slm) and ml.

(G and H) Small oligomeric forms of Aβ were detected by immunoprecipitation/western blotting in different brain regions of 13-month-old EC-APP and hAPP-J20 mice. Aβ dimers were present in all brain regions analyzed; the highest levels were in the EC of EC-APP mice. Syn., synthetic.

Therefore, we measured LTP and baseline synaptic transmission in mice with well-developed cognitive deficits. We first tested a new cohort of 13- to 14-month-old NTG and EC-APP mice in the MWM and replicated the learning and memory deficits described in Figure 2 (data not shown). In EC-APP mice with verified spatial learning deficits, baseline synaptic transmission strength was reduced only at the Schaffer collateral to CA1 synapses (Figures 6E and 6F). As in hAPP-J20 mice, LTP was depressed at the perforant path to GC synapses in EC-APP mice relative to NTG controls, but no LTP deficits were identified in CA1 (Figures 6G and 6H).

Aβ Deposition in EC-APP Mice

Molecular alterations in DG GCs of EC-APP mice could result from direct actions of presynaptically released Aβ on postsynaptic membranes or from functional changes in afferent input from perforant path axons caused by Aβ in EC neurons. To address these nonexclusive possibilities, we determined whether Aβ was present not only in the EC, but also in terminal projection zones of EC layer II/III neurons, which overexpress APP/Aβ in EC-APP mice. Soluble Aβ was measured by ELISA in microdissected brain regions of young EC-APP mice before plaque deposition and compared to hAPP-J20 mice. EC-APP mice had high levels of Aβ1-x and Aβ1-42 in the EC (Figure 7A) and relatively high levels of Aβ1-x in the DG

(Figure 7B), comparable to those of hAPP-J20 mice, which have much higher APP levels in the DG (Figures S1C and S1D). In contrast, levels of Aβ1-42 in the DG (Figure 7B) and of Aβ1-x and Aβ1-42 in the CA1 region (Figure 7C) were lower in EC-APP mice than in hAPP-J20 mice. EC-APP mice had higher levels of soluble Aβ in EC and DG, but not in CA regions (Figures S3C–S3E), than singly transgenic tet-APP mice. Therefore, the low levels of Aβ in the CA of young EC-APP mice were likely caused by leakiness of the tet promoter.

At 6 months of age, EC-APP mice had Aβ-immunoreactive deposits in the EC and the RC, but not in other cortical areas or in the DG (Figure 7D). By 13 months, Aβ deposition had increased markedly in the EC and RC and in the DG and CA regions of the hippocampus. Aβ deposition also increased in the PC, which is near the RC (Figures 7E and 7F). The extent of Aβ deposition in the EC and RC was comparable and significantly higher than in other regions analyzed. Aβ deposits were found in all layers in the EC (Figure 7F, left) and primarily in perforant pathway terminal fields in the hippocampus: the stratum lacunosum moleculare (Figure 7F, middle) and the molecular layer of the DG (Figure 7F, right). Aβ deposits were minimal or absent in the hilus and mossy fiber pathway. In contrast, hAPP-J20 mice had particularly prominent deposits in the inner molecular layer of the DG and mossy fiber pathway in CA3 (Figure S6). This pattern of deposition in EC-APP mice strongly suggests presynaptic release of Aβ, as opposed to simple diffusion from the EC.

Finally, we measured the levels of smaller, potentially more toxic oligomeric Aβ assemblies in 13-month-old EC-APP mice by immunoprecipitation and western blotting. The intensity of bands corresponding to Aβ dimers was most intense in EC, intermediate in DG, and lowest in CA1 (Figures 7G and 7H). Aβ dimer levels in DG were similar in EC-APP and hAPP-J20 mice (Figure 7G), but Aβ monomer levels in DG and CA1 were lower in EC-APP mice.

Reducing Aβ Production by γ-Secretase Inhibition Reverses an Abnormal Behavior in EC-APP Mice

Much evidence suggests that Aβ is the primary mediator of AD-related molecular and behavioral abnormalities in APP transgenic mice and humans (Harris et al., 2010; Palop et al., 2003, 2007; Sun et al., 2008; Tanzi, 2005; Walsh and Selkoe, 2004). However, other APP metabolites or the holoprotein itself could also have a role. Therefore, we analyzed the behavioral effects of LY-411575, a γ-secretase inhibitor (GSI) that rapidly reduces tissue and interstitial fluid levels of Aβ in APP transgenic mice (Abramowski et al., 2008; Cirrito et al., 2003; Lanz et al., 2004). Four-month-old EC-APP and NTG mice were treated once daily for 2 days and tested in the elevated plus maze because it is a quick and sensitive test of dysfunction in this line (Figures 3 and 8A), and chronic treatment with this GSI causes mice to become too ill for long-term behavioral experiments such as the MWM (L.V. and J.J.P., unpublished data). LY-411575-treated EC-APP mice spent significantly less time in the open arms than vehicle-treated EC-APP mice, normalizing their behavior in this test as compared with vehicle-treated NTG controls (Figure 8A). There was a trend toward increased open arm time in GSI-treated NTG mice versus vehicle-treated NTG controls, but this difference was not statistically significant.

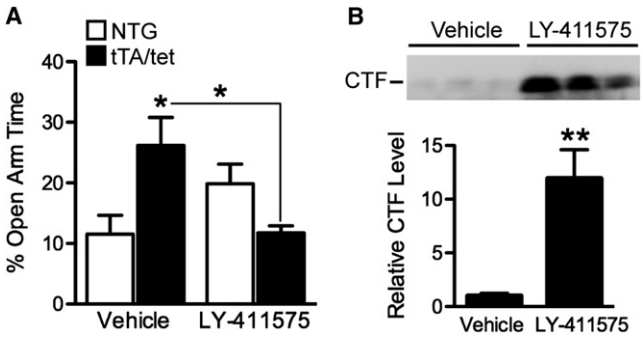

Figure 8. Inhibiting γ-Secretase Cleavage to Reduce Aβ Production Normalizes EPM Behavior in 4-Month-Old EC-APP Mice

(A) Mice were injected once a day with LY-411575 (3 mg/kg) or vehicle on 2 consecutive days and tested in the EPM 6–8 hr after the second injection. Vehicle-treated EC-APP (tTA/tet) mice spent more time in the open arms than vehicle-treated NTG mice. LY-411575 treatment significantly reduced the time EC-APP mice spent in the open arms to levels in vehicle-treated NTG controls. n = 5–7 mice/group. $p < 0.005$ for the interaction effect between genotype and treatment by two-way ANOVA, *$p < 0.05$ versus NTG + vehicle or as indicated by bracket (one-way ANOVA followed by Tukey post hoc test).

(B) APP CTFs in the EC of EC-APP mice were measured by western blotting and quantified by densitometry. Inhibition of γ-secretase cleavage increased CTF levels. n = 5–7 mice/group. **$p < 0.005$ versus vehicle by t test. Values are mean ± SEM.

We verified that LY-411575 was active by measuring C-terminal fragments (CTFs) in the EC, which increase when γ-secretase is inhibited (Abramowski et al., 2008; Cirrito et al., 2003). Ten hours after the second injection of LY-411575, CTF levels were significantly increased (Figure 8B). Therefore, it is very unlikely that β-secretase-cleaved CTFs such as C99 underlie this behavioral abnormality in APP transgenic mice. Measurements of Aβ levels were not used as a reporter for LY-411575 activity because mice at this age already have Aβ deposition in the EC, and existing plaques are not reduced by LY-411575 (Garcia-Alloza et al., 2009).

DISCUSSION

It is not known how EC dysfunction contributes to cognitive decline in AD or whether early vulnerability of the EC initiates the spread of dysfunction through interconnected neural networks. To address these questions, we studied transgenic mice with spatially restricted overexpression of mutant APP primarily in superficial-layer neurons of the EC. We found age-dependent deficits in learning and memory, other behavioral alterations, and aberrant synchronization in distant cortical networks in these mice. We also found that Aβ-induced molecular and functional impairments can cross synapses, progressing with time/aging initially from EC neurons to GCs in the DG and then to pyramidal neurons in CA1. Our data directly support the hypothesis that AD-related neuronal dysfunction is propagated through synaptically connected neural networks, with the EC as an important hub region of early vulnerability.

Potential Involvement of the Retrosplenial Cortex

In AD, PiB-PET and fMRI studies demonstrated extensive Aβ deposition in the "default mode network" (DMN), a group of brain regions with correlative activity that deactivate during cognitive tasks (Buckner et al., 2005; Sperling et al., 2009). A major hub of the DMN is the posterior cingulate cortex, which includes the RC in humans and nonhuman primates (Vann et al., 2009). We also found extensive Aβ deposition in the RC of EC-APP mice, which was not different from that in the EC, even though APP overexpression was much lower in the RC than the EC (Figure 1). hAPP-J20 mice also had substantial Aβ deposition in the RC (Figure S6).

The RC has reciprocal connections to the medial EC (Jones and Witter, 2007; Van Groen and Wyss, 2003; Wyss and Van Groen, 1992), but inputs from the medial EC originate in neurons of deeper layers (Insausti et al., 1997), not in neurons of superficial layers, which express mutant APP in the EC-APP mouse model. Thus, the EC is an unlikely source of Aβ deposition in the RC of these mice. EC-APP mice also express mutant APP in the parahippocampal pre- and parasubiculum, which have reciprocal connections to the RC (Jones and Witter, 2007; Van Groen and Wyss, 2003; Wyss and Van Groen, 1992). Therefore, presynaptic terminals from these regions may release Aβ into the RC. The RC also receives hippocampal input directly from the subiculum, but does not share direct projections with the DG, CA1, or CA3, at least in rats (Jones and Witter, 2007; Van Groen and Wyss, 2003; Wyss and Van Groen, 1992). In light of these anatomical connections, neurons of the RC could also be affected indirectly by Aβ-induced alterations in the activity of the EC-hippocampal network. Indeed, lesions of the hippocampus reduce immediate-early gene expression in the RC (Albasser et al., 2007).

In conjunction with the hippocampus, the RC is important in spatial navigation, learning, and memory (Vann et al., 2009). Therefore, accumulation of pathogenic Aβ assemblies in the RC could contribute directly to deficits in these functions. Importantly, the EC, RC, and hippocampus are part of a broader network regulating spatial learning and memory, and dysfunction in one region is not necessarily independent of dysfunction in the others.

Transsynaptic Effects of Aβ

Lesions of the EC or transecting the perforant pathway reduces Aβ deposition in the DG of transgenic APP/PS1 mice (Lazarov et al., 2002; Sheng et al., 2002). These studies support the hypothesis that the EC is a primary source of Aβ in the hippocampus. However, since neuronal activity increases Aβ production (Cirrito et al., 2005, 2008; Kamenetz et al., 2003), reduced Aβ deposition in the DG after perforant pathway lesions might also result from decreased stimulation of GCs in the DG and commensurate decreases in their activity and Aβ production. Our data directly demonstrate that perforant pathway axons are an important source of Aβ in the DG, as APP expression in EC-APP mice was seen in the EC and perforant path but not in DG GCs. These findings are consistent with data suggesting that presynaptic terminals are a key site for Aβ production and release (Buxbaum et al., 1998; Wei et al., 2010).

Aβ released from perforant pathway terminals may act directly on postsynaptic cells and alter their functions, particularly when aggregated in oligomeric assemblies. Alternatively, Aβ may affect the presynaptic terminals themselves, for instance, by altering the release probability of synaptic vesicles (Abramov et al., 2009) and thus changing downstream signaling pathways in the postsynaptic GCs. In addition, Aβ synthesized and released from cell bodies or dendrites of EC neurons may act on these very cells, altering afferent input to the DG. These possibilities are not mutually exclusive and deserve to be explored in future studies. The reduction in synaptic activity-related proteins in DG GCs probably reflects altered network properties and could have detrimental effects on hippocampal function. For example, reducing calbindin or Fos levels in normal rats or mice causes deficits in spatial learning (He et al., 2002; Molinari et al., 1996); decreased levels of synaptophysin suggest loss or impairment of presynaptic terminals that could disrupt communication between the EC and DG (Hsia et al., 1999; Scheff and Price, 2003; Terry et al., 1991).

Regardless of whether Aβ exerts its main effects in the EC, DG, or both, the progression of molecular and functional synaptic alterations from EC neurons to DG neurons and CA1 neurons supports the hypothesis that AD progresses through synaptically connected neural networks and that this process could be triggered by Aβ (Braak et al., 2006; Buckner et al., 2005; Palop and Mucke, 2010; Seeley et al., 2009; Sperling et al., 2009). The propagation of functional alterations into the DG and CA1 is likely to be very rapid, whereas molecular and structural changes may require more time to develop, as suggested by the delayed decrease in synaptophysin levels in CA1. Whether APP/Aβ expression in the EC exerts indirect effects on DG target cells in the hilus or CA3 region remains to be determined.

Similarities between hippocampal synaptic deficits in hAPP-J20 mice with high levels of Aβ in DG and CA1 and in EC-APP mice with lower levels of Aβ in these regions suggest two possibilities. First, the deficits may emerge whenever Aβ levels exceed a threshold. In support of this possibility, synaptic transmission deficits in CA1 are also present in hAPP-J9 mice, whose hippocampal hAPP/Aβ levels are half those in hAPP-J20 mice (Hsia et al., 1999; Mucke et al., 2000). Aβ levels in the DG of EC-APP mice (i.e., Aβ released from EC-derived terminals) are ~70% of those in hAPP-J20 mice (Figure 7B). Second, the deficits in the hippocampus of both lines may be caused indirectly by Aβ-induced abnormalities in the activity of EC neurons. These possibilities are not mutually exclusive. The detection of epileptiform activity in the PC of EC-APP mice suggests that APP/Aβ in one area may impact other brain regions by causing aberrant activity patterns that rapidly spread through interconnected neural networks.

Aβ is released from presynaptic terminals (Wei et al., 2010) and, in our opinion, is the likeliest APP metabolite to mediate transsynaptic spread of AD. The caspase-generated APP-C31 fragment (Gervais et al., 1999; Weidemann et al., 1999) does not play a major role in the development of AD-related abnormalities in APP transgenic mice (Harris et al., 2010). Treatment with LY-411575, a GSI that decreases soluble Aβ levels and increases CTF levels (Figure 8B) (Abramowski et al., 2008; Cirrito et al., 2003; Lanz et al., 2004), reversed behavioral abnormalities in EC-APP mice. This finding supports a critical role of Aβ and makes it very unlikely that the abnormal behavior of EC-APP

mice was caused by β-secretase-cleaved CTFs such as C99. However, it does not exclude potential contributions from all other APP metabolites that might have copathogenic effects, including N-APP (Nikolaev et al., 2009) and AICD (Ghosal et al., 2009).

Role of the EC in Cognitive and Noncognitive Behaviors

Although the relationship between cognitive and behavioral abnormalities in APP transgenic mice and humans with AD is a matter of debate, we previously identified prominent navigational and hippocampal deficits in both the models and in AD patients (delpolyi et al., 2007, 2008). In the current study, increasing Aβ production by EC neurons and perhaps also by RC neurons caused age-dependent deficits in spatial learning and memory, suggesting that impairments of those neurons or their target regions are critical for the functional deficits. Indeed, the EC and its intact perforant path connections to the hippocampus are critical for learning, retrieval, and/or consolidation of spatial memory (Kirkby and Higgins, 1998; Ramirez et al., 2007; Remondes and Schuman, 2004; Steffenach et al., 2005). Aβ-induced dysfunction of the RC could also contribute to these behavioral deficits.

The reversal-learning paradigm (Figures 2G and 2H) provides evidence for a specific role of the EC and its connections in flexible learning of a new spatial task. This task requires mice to discard a previously learned target location and acquire a new one. EC-APP mice had difficulties learning the new platform location. The learning deficits in the initial component of the MWM complicate the interpretation of this phenotype as solely a reversal-learning deficit. However, while EC-APP mice did not show significant memory retention in the first task, they showed some evidence of learning to navigate to the hidden platform initially (Figure 2C, $p = 0.06$, one-way ANOVA effect of time). The lack of any improvement in the reversal-learning task suggests an additional impairment in flexibility or reflects other behavioral disturbances. The EC-APP model could help elucidate the roles of the EC and perforant pathway projections in this process.

Mice of the APP transgenic line PDAPP 109 were also impaired in a related behavioral task (Chen et al., 2000). Neither the anatomical regions nor the molecular mechanisms underlying the required flexibility have been elucidated, although adult neurogenesis in the DG is important for spatial reversal learning (Garthe et al., 2009) and is altered in APP transgenic mice (Donovan et al., 2006; López-Toledano and Shelanski, 2007; Sun et al., 2009), most likely because Aβ causes an imbalance in excitatory and inhibitory inputs to newborn GCs (Sun et al., 2009).

EC-APP mice also behaved abnormally in the elevated plus maze and were hyperactive in the Y-maze. Time spent in the open arms of an elevated plus maze is usually considered a measure of anxiety, and with this interpretation, several lines of hAPP mice appear to be less anxious (Cheng et al., 2007; Chin et al., 2005; Harris et al., 2010; Ognibene et al., 2005). Increased time in the open arms could also reflect disinhibition in APP transgenic mice. The amygdala, regarded as the anatomical substrate of fear- and anxiety-related behaviors, receives direct input from the EC. However, this input is from neurons in deep cortical layers (McDonald, 1998), which do not overexpress mutant APP in the EC-APP mice. The ventral hippocampus is more specifically associated with performance in the elevated plus maze than the amygdala (Bannerman et al., 2004) and receives direct input from the superficial-layer neurons overexpressing mutant APP in EC-APP mice. Like EC-APP mice, rats with lesions of the ventral hippocampus or severed perforant pathway projections to the ventral hippocampus spent more time in the open arms of an elevated plus maze (Kjelstrup et al., 2002; Steffenach et al., 2005). Our data further support a role for the EC and its hippocampal connections in this behavioral phenotype, although the amygdala could still be involved in a more indirect fashion.

The hippocampus may be one of many brain regions that can regulate locomotor activity (Bast and Feldon, 2003). Unlike APP transgenic mice with widespread transgene expression, which are hyperactive in both the open field and the Y-maze (Chin et al., 2005; Kobayashi and Chen, 2005; Roberson et al., 2007), EC-APP mice were hyperactive only in the Y-maze. Why EC-APP mice performed differently in these tests is unclear. One possibility is that these tests measure different components of locomotor activity control. Indeed, all groups of mice habituated to the open field but not to the Y-maze. Activity in the open field may be related to hippocampus-dependent information gathering about a novel environment, whereas locomotor activity in the Y-maze may reflect a different process.

Therapeutic Implications

Without effective drug treatments for AD, interest in alternative approaches, such as gene therapy and stem cells, is increasing (Spencer et al., 2007; Tuszynski et al., 2005). However, the success of these approaches may depend on whether AD affects multiple brain regions in parallel or in sequence. In the latter case, AD progression might be stopped by targeting the specific region in which the disease originates, which would be simpler than targeting multiple regions. Thus, if dysfunction in the EC leads to the propagation of AD across synapses throughout a neural network, early interference, specifically in the EC, might be of therapeutic benefit, perhaps halting disease progression. Indeed, BDNF introduced into the EC was transported into the hippocampus and rescued spatial memory functions in APP transgenic mice (Nagahara et al., 2009). Tau and Aβ may also share features with prions, including the ability to propagate pathological protein aggregation, perhaps through synaptic connections (Clavaguera et al., 2009; Eisele et al., 2009; Frost and Diamond, 2010). It will be interesting to assess the effects of selective EC expression of tau and other factors on the development and propagation of AD-related pathologies.

EXPERIMENTAL PROCEDURES

Animals

Neuropsin-tTA heterozygous transgenic mice (Yasuda and Mayford, 2006) were crossed with tet-APP heterozygous transgenic mice (Jankowsky et al., 2005) to generate four genotypes: tTA/tet doubly transgenic (EC-APP) mice, tTA or tet singly transgenic mice, and NTG controls. Mice did not receive doxycycline so as to maintain expression of the tet-APP transgene. Neuropsin-tTA mice on the C57BL/6 background were provided by Mark Mayford. Tet-APP mice were on a C57BL/6-C3H background (Jackson Laboratory,

stock no. 006004) or on a C57BL/6 background (Jackson Laboratory, stock no. 007049). See Supplemental Experimental Procedures for more detail on strain background. All analyses were done in gender-balanced groups. Experimenters were blinded to genotype and treatment. The Institutional Animal Care and Use Committee of the University of California, San Francisco approved all experiments.

Behavioral Tests

One cohort of mice was evaluated at 4, 9, and 13 months of age in the elevated plus maze and MWM. The same mice were analyzed in the Y-maze at 9 and 13 months.

Elevated Plus Maze

The elevated plus maze consisted of two open (without walls) and two enclosed (with walls) arms elevated 63 cm above the ground (Hamilton-Kinder). Mice were allowed to habituate in the testing room under dim light for 1 hr before testing. During testing, mice were placed at the junction between the open and closed arms of the plus maze and allowed to explore for 5 min. The maze was cleaned with 70% alcohol after testing of each mouse. Total distance traveled and time spent in the open and closed arms were calculated based on infrared photobeam breaks.

Y-Maze

The apparatus consisted of three symmetrical arms in a Y shape. Before testing, mice were transferred to the testing room and acclimated for at least 1 hr. During testing, each mouse was placed in a starting arm facing the wall. Arm entries were recorded for 6 min, divided into six 1 min intervals. The maze was cleaned with 70% alcohol between testing of each mouse. Spontaneous alternations and total activity were calculated.

Morris Water Maze

Mice were trained in the MWM for 3–5 days as described, with modifications (Harris et al., 2010). See Supplemental Experimental Procedures for details. At 13 months of age, mice also underwent reversal training, where the target platform was moved to the opposite quadrant of the MWM pool after the initial hidden training sessions were completed. Behavior was recorded with a video tracking system (Noldus). Escape latencies, distance traveled, swim paths, swim speeds, percent time spent in each quadrant, and platform crossings were recorded for subsequent analysis. Thigmotaxis was monitored during the last trial of hidden platform training in both initial acquisition and reversal learning. No mice exhibited thigmotaxis in these experiments. Floating behavior was also monitored during training. Only one mouse (a singly tTA transgenic at 13 months) exhibited floating and was removed from the analysis.

γ-Secretase Inhibitor Treatment

NTG and EC-APP mice were injected subcutaneously once daily for 2 days with 3 mg/kg LY-411575 (a gift of J. Tung and the Myelin Repair Foundation) or vehicle (corn oil) and tested in the elevated plus maze 6–8 hr after the last injection. All mice were sacrificed directly after the testing (approximately 10 hr from the second LY-411575 injection). Brains were harvested and frozen for ELISA and western blot analyses.

Immunohistochemistry

Tissue was prepared as described (Harris et al., 2010). Primary antibodies were rabbit anti-calbindin (1:20,000; Swant), rabbit anti-Fos (1:10,000; Ab-5, Oncogene), rabbit anti-NPY (1:8000; Immunostar), mouse biotinylated anti-Aβ (1:400; 3D6, Elan Pharmaceuticals), mouse anti-APP/Aβ (1:10,000; clone 6E10; Covance), mouse anti-hAPP (1:2000, clone 8E5, Elan Pharmaceuticals), and mouse anti-synaptophysin (1:1000; Boehringer Mannheim). Sections labeled with anti-synaptophysin were incubated with FITC-conjugated horse anti-mouse IgG secondary antibody (1:75; Vector). Binding of other primary antibodies was detected with biotinylated donkey anti-rabbit or anti-mouse (1:1000; Jackson Immunoresearch), followed by incubation with avidin-biotin complex (Vector). Fos, calbindin, NPY, synaptophysin, and Aβ immunoreactivities were quantified in a behaviorally naive cohort of mice at 6 months and in mice that underwent behavioral testing at 13 months of age. Quantifications were performed as described (Chin et al., 2004; Palop et al., 2003, 2007).

Aβ ELISAs and Immunoblotting

For Aβ and APP measurements in specific regions, brain tissues were microdissected into DG, EC, CA, and RC. To obtain DG samples, the GC and molecular layers were microdissected away from the hilar region and CA3. For Aβ ELISAs, samples were snap-frozen and homogenized in 5 M guanidine buffer. Aβ1-x (approximates total Aβ) and Aβ1-42 were quantified as described (Johnson-Wood et al., 1997; Mucke et al., 2000). Low-molecular-weight oligomeric Aβ species were detected by immunoprecipitation and western blotting. APP levels were assessed by western blotting in microdissected samples as described (Harris et al., 2010). See Supplemental Experimental Procedures for further details.

EEG Recordings

Mice were implanted for video EEG monitoring after anesthesia with intraperitoneal ketamine (75 mg/kg) and medetomidine (1 mg/kg). Teflon-coated silver wire electrodes (0.125 mm diameter) soldered to a multichannel electrical connector were implanted into the subdural space over the left frontal cortex (coordinates relative to the bregma were M/L, ±1; A/P, ±1) and the left and right PC (M/L, ±2, A/P, −2). The left frontal cortex electrode was used as a reference. All EEG recordings were carried out at least 10 days after surgery on freely moving mice in a recording chamber. EEG activity was recorded with the Harmonie software (version 5.0b) for 24 hr. The number of SWDs was automatically detected by the Gotman spike and seizure detectors (Harmonie) and manually verified.

Electrophysiological Recordings in Acute Slices

Acute coronal slices (400 μm) were prepared from NTG and EC-APP mice at 6 and 14 months of age. See Supplemental Experimental Procedures for details. fEPSPs were recorded with glass electrodes (~3 MΩ tip resistance) filled with 1 M NaCl and 25 mM HEPES (pH 7.3) and evoked every 20 s with a bipolar tungsten electrode (FHC, Inc.) in the presence of 50 μM picrotoxin (Tocris). Recordings were filtered at 2 kHz (−3 dB, eight-pole Bessel), digitally sampled at 20 kHz with a Multiclamp 700A amplifier (Molecular Devices), and acquired with a Digidata-1322A digitizer and pClamp 9.2 software. Synaptic transmission strengths in the DG and CA1 were assessed by generating input-output (I-O) curves for fEPSPs. Fiber volley amplitude and initial slope of the fEPSP responses to a range of stimulation from 25 to 800 μA were recorded, and a response curve was generated for both values. Stimulus strength was adjusted to ~30% of the maximal fEPSP response for recordings that followed. After a 10 min stable baseline was established, LTP was induced in CA1 by high-frequency stimulation (four 100 Hz trains of 100 stimuli every 20 s) and in DG by theta burst stimulation (ten bursts repeated ten times every 15 s; each burst consisting of four pulses at 100 Hz was repeated at 5 Hz).

Statistical Analyses

Experimenters were blinded to the genotype and treatment of mice. Statistical analyses were conducted with GraphPad Prism version 4.0 or 5.0. Differences between means were analyzed by two-tailed t test and one-way or two-way ANOVA with post hoc tests as appropriate; $p < 0.05$ was considered significant.

SUPPLEMENTAL INFORMATION

Supplemental Information includes Supplemental Experimental Procedures, Supplemental References, and six figures and can be found with this article online at doi:10.1016/j.neuron.2010.10.020.

ACKNOWLEDGMENTS

This work was supported in part by NIH grants AG011385 and AG022074 to L.M. and a fellowship from the McBean Foundation to J.A.H. We thank Mark Mayford for providing neuropsin-tTA mice, David Borchelt for donating the tet-APP mice to Jackson Laboratory, M. Howard for help with

electrophysiological recordings, X. Wang and H. Solanoy for technical support, S. Ordway for editorial review, and M. De la Cruz for administrative assistance.

Accepted: September 3, 2010
Published: November 3, 2010

REFERENCES

Abramov, E., Dolev, I., Fogel, H., Ciccotosto, G.D., Ruff, E., and Slutsky, I. (2009). Amyloid-beta as a positive endogenous regulator of release probability at hippocampal synapses. Nat. Neurosci. *12*, 1567–1576.

Abramowski, D., Wiederhold, K.H., Furrer, U., Jaton, A.L., Neuenschwander, A., Runser, M.J., Danner, S., Reichwald, J., Ammaturo, D., Staab, D., et al. (2008). Dynamics of Abeta turnover and deposition in different beta-amyloid precursor protein transgenic mouse models following gamma-secretase inhibition. J. Pharmacol. Exp. Ther. *327*, 411–424.

Albasser, M.M., Poirier, G.L., Warburton, E.C., and Aggleton, J.P. (2007). Hippocampal lesions halve immediate-early gene protein counts in retrosplenial cortex: distal dysfunctions in a spatial memory system. Eur. J. Neurosci. *26*, 1254–1266.

Bannerman, D.M., Rawlins, J.N., McHugh, S.B., Deacon, R.M., Yee, B.K., Bast, T., Zhang, W.N., Pothuizen, H.H., and Feldon, J. (2004). Regional dissociations within the hippocampus—memory and anxiety. Neurosci. Biobehav. Rev. *28*, 273–283.

Bast, T., and Feldon, J. (2003). Hippocampal modulation of sensorimotor processes. Prog. Neurobiol. *70*, 319–345.

Belzung, C., and Griebel, G. (2001). Measuring normal and pathological anxiety-like behaviour in mice: a review. Behav. Brain Res. *125*, 141–149.

Blennow, K., de Leon, M.J., and Zetterberg, H. (2006). Alzheimer's disease. Lancet *368*, 387–403.

Braak, H., and Braak, E. (1991). Neuropathological stageing of Alzheimer-related changes. Acta Neuropathol. *82*, 239–259.

Braak, H., Rüb, U., Schultz, C., and Del Tredici, K. (2006). Vulnerability of cortical neurons to Alzheimer's and Parkinson's diseases. J. Alzheimers Dis. *9* (*Suppl 3*), 35–44.

Buckner, R.L., Snyder, A.Z., Shannon, B.J., LaRossa, G., Sachs, R., Fotenos, A.F., Sheline, Y.I., Klunk, W.E., Mathis, C.A., Morris, J.C., and Mintun, M.A. (2005). Molecular, structural, and functional characterization of Alzheimer's disease: evidence for a relationship between default activity, amyloid, and memory. J. Neurosci. *25*, 7709–7717.

Buxbaum, J.D., Thinakaran, G., Koliatsos, V., O'Callahan, J., Slunt, H.H., Price, D.L., and Sisodia, S.S. (1998). Alzheimer amyloid protein precursor in the rat hippocampus: transport and processing through the perforant path. J. Neurosci. *18*, 9629–9637.

Chen, G., Chen, K.S., Knox, J., Inglis, J., Bernard, A., Martin, S.J., Justice, A., McConlogue, L., Games, D., Freedman, S.B., and Morris, R.G. (2000). A learning deficit related to age and β-amyloid plaques in a mouse model of Alzheimer's disease. Nature *408*, 975–979.

Cheng, I.H., Scearce-Levie, K., Legleiter, J., Palop, J.J., Gerstein, H., Bien-Ly, N., Puoliväli, J., Lesné, S., Ashe, K.H., Muchowski, P.J., and Mucke, L. (2007). Accelerating amyloid-β fibrillization reduces oligomer levels and functional deficits in Alzheimer disease mouse models. J. Biol. Chem. *282*, 23818–23828.

Chin, J., Palop, J.J., Yu, G.-Q., Kojima, N., Masliah, E., and Mucke, L. (2004). Fyn kinase modulates synaptotoxicity, but not aberrant sprouting, in human amyloid precursor protein transgenic mice. J. Neurosci. *24*, 4692–4697.

Chin, J., Palop, J.J., Puoliväli, J., Massaro, C., Bien-Ly, N., Gerstein, H., Scearce-Levie, K., Masliah, E., and Mucke, L. (2005). Fyn kinase induces synaptic and cognitive impairments in a transgenic mouse model of Alzheimer's disease. J. Neurosci. *25*, 9694–9703.

Cirrito, J.R., May, P.C., O'Dell, M.A., Taylor, J.W., Parsadanian, M., Cramer, J.W., Audia, J.E., Nissen, J.S., Bales, K.R., Paul, S.M., et al. (2003). In vivo assessment of brain interstitial fluid with microdialysis reveals plaque-associated changes in amyloid-beta metabolism and half-life. J. Neurosci. *23*, 8844–8853.

Cirrito, J.R., Yamada, K.A., Finn, M.B., Sloviter, R.S., Bales, K.R., May, P.C., Schoepp, D.D., Paul, S.M., Mennerick, S., and Holtzman, D.M. (2005). Synaptic activity regulates interstitial fluid amyloid-β levels in vivo. Neuron *48*, 913–922.

Cirrito, J.R., Kang, J.E., Lee, J., Stewart, F.R., Verges, D.K., Silverio, L.M., Bu, G., Mennerick, S., and Holtzman, D.M. (2008). Endocytosis is required for synaptic activity-dependent release of amyloid-beta in vivo. Neuron *58*, 42–51.

Clavaguera, F., Bolmont, T., Crowther, R.A., Abramowski, D., Frank, S., Probst, A., Fraser, G., Stalder, A.K., Beibel, M., Staufenbiel, M., et al. (2009). Transmission and spreading of tauopathy in transgenic mouse brain. Nat. Cell Biol. *11*, 909–913.

delpolyi, A.R., Rankin, K.P., Mucke, L., Miller, B.L., and Gorno-Tempini, M.L. (2007). Spatial cognition and the human navigation network in AD and MCI. Neurology *69*, 986–997.

delpolyi, A.R., Fang, S., Palop, J.J., Yu, G.-Q., Wang, X., and Mucke, L. (2008). Altered navigational strategy use and visuospatial deficits in hAPP transgenic mice. Neurobiol. Aging *29*, 253–266.

Donovan, M.H., Yazdani, U., Norris, R.D., Games, D., German, D.C., and Eisch, A.J. (2006). Decreased adult hippocampal neurogenesis in the PDAPP mouse model of Alzheimer's disease. J. Comp. Neurol. *495*, 70–83.

Eichenbaum, H., and Lipton, P.A. (2008). Towards a functional organization of the medial temporal lobe memory system: role of the parahippocampal and medial entorhinal cortical areas. Hippocampus *18*, 1314–1324.

Eisele, Y.S., Bolmont, T., Heikenwalder, M., Langer, F., Jacobson, L.H., Yan, Z.X., Roth, K., Aguzzi, A., Staufenbiel, M., Walker, L.C., and Jucker, M. (2009). Induction of cerebral beta-amyloidosis: intracerebral versus systemic Abeta inoculation. Proc. Natl. Acad. Sci. USA *106*, 12926–12931.

Frost, B., and Diamond, M.I. (2010). Prion-like mechanisms in neurodegenerative diseases. Nat. Rev. Neurosci. *11*, 155–159.

Galvan, V., Gorostiza, O.F., Banwait, S., Ataie, M., Logvinova, A.V., Sitaraman, S., Carlson, E., Sagi, S.A., Chevallier, N., Jin, K., et al. (2006). Reversal of Alzheimer's-like pathology and behavior in human APP transgenic mice by mutation of Asp664. Proc. Natl. Acad. Sci. USA *103*, 7130–7135.

Games, D., Adams, D., Alessandrini, R., Barbour, R., Berthelette, P., Blackwell, C., Carr, T., Clemens, J., Donaldson, T., Gillespie, F., et al. (1995). Alzheimer-type neuropathology in transgenic mice overexpressing V717F β-amyloid precursor protein. Nature *373*, 523–527.

Garcia-Alloza, M., Subramanian, M., Thyssen, D., Borrelli, L.A., Fauq, A., Das, P., Golde, T.E., Hyman, B.T., and Bacskai, B.J. (2009). Existing plaques and neuritic abnormalities in APP:PS1 mice are not affected by administration of the gamma-secretase inhibitor LY-411575. Mol. Neurodegener. *4*, 19.

Garthe, A., Behr, J., and Kempermann, G. (2009). Adult-generated hippocampal neurons allow the flexible use of spatially precise learning strategies. PLoS ONE *4*, e5464.

Gervais, F.G., Xu, D., Robertson, G.S., Vaillancourt, J.P., Zhu, Y., Huang, J., LeBlanc, A., Smith, D., Rigby, M., Shearman, M.S., et al. (1999). Involvement of caspases in proteolytic cleavage of Alzheimer's amyloid-β precursor protein and amyloidogenic A β peptide formation. Cell *97*, 395–406.

Ghosal, K., Vogt, D.L., Liang, M., Shen, Y., Lamb, B.T., and Pimplikar, S.W. (2009). Alzheimer's disease-like pathological features in transgenic mice expressing the APP intracellular domain. Proc. Natl. Acad. Sci. USA *106*, 18367–18372.

Gómez-Isla, T., Price, J.L., McKeel, D.W., Jr., Morris, J.C., Growdon, J.H., and Hyman, B.T. (1996). Profound loss of layer II entorhinal cortex neurons occurs in very mild Alzheimer's disease. J. Neurosci. *16*, 4491–4500.

Götz, J., Streffer, J.R., David, D., Schild, A., Hoerndli, F., Pennanen, L., Kurosinski, P., and Chen, F. (2004). Transgenic animal models of Alzheimer's disease and related disorders: histopathology, behavior and therapy. Mol. Psychiatry *9*, 664–683.

Harris, J.A., Devidze, N., Halabisky, B., Lo, I., Thwin, M.T., Yu, G.Q., Bredesen, D.E., Masliah, E., and Mucke, L. (2010). Many neuronal and behavioral

impairments in transgenic mouse models of Alzheimer's disease are independent of caspase cleavage of the amyloid precursor protein. J. Neurosci. *30*, 372–381.

He, J., Yamada, K., and Nabeshima, T. (2002). A role of Fos expression in the CA3 region of the hippocampus in spatial memory formation in rats. Neuropsychopharmacology *26*, 259–268.

Hsia, A.Y., Masliah, E., McConlogue, L., Yu, G.Q., Tatsuno, G., Hu, K., Kholodenko, D., Malenka, R.C., Nicoll, R.A., and Mucke, L. (1999). Plaque-independent disruption of neural circuits in Alzheimer's disease mouse models. Proc. Natl. Acad. Sci. USA *96*, 3228–3233.

Hsiao, K., Chapman, P., Nilsen, S., Eckman, C., Harigaya, Y., Younkin, S., Yang, F.S., and Cole, G. (1996). Correlative memory deficits, Abeta elevation, and amyloid plaques in transgenic mice. Science *274*, 99–102.

Insausti, R., Herrero, M.T., and Witter, M.P. (1997). Entorhinal cortex of the rat: cytoarchitectonic subdivisions and the origin and distribution of cortical efferents. Hippocampus *7*, 146–183.

Jankowsky, J.L., Slunt, H.H., Gonzales, V., Savonenko, A.V., Wen, J.C., Jenkins, N.A., Copeland, N.G., Younkin, L.H., Lester, H.A., Younkin, S.G., and Borchelt, D.R. (2005). Persistent amyloidosis following suppression of Abeta production in a transgenic model of Alzheimer disease. PLoS Med. *2*, e355.

Johnson-Wood, K., Lee, M., Motter, R., Hu, K., Gordon, G., Barbour, R., Khan, K., Gordon, M., Tan, H., Games, D., et al. (1997). Amyloid precursor protein processing and A β_{42} deposition in a transgenic mouse model of Alzheimer disease. Proc. Natl. Acad. Sci. USA *94*, 1550–1555.

Jones, B.F., and Witter, M.P. (2007). Cingulate cortex projections to the parahippocampal region and hippocampal formation in the rat. Hippocampus *17*, 957–976.

Kamenetz, F., Tomita, T., Hsieh, H., Seabrook, G., Borchelt, D., Iwatsubo, T., Sisodia, S., and Malinow, R. (2003). APP processing and synaptic function. Neuron *37*, 925–937.

Kirkby, D.L., and Higgins, G.A. (1998). Characterization of perforant path lesions in rodent models of memory and attention. Eur. J. Neurosci. *10*, 823–838.

Kjelstrup, K.G., Tuvnes, F.A., Steffenach, H.A., Murison, R., Moser, E.I., and Moser, M.B. (2002). Reduced fear expression after lesions of the ventral hippocampus. Proc. Natl. Acad. Sci. USA *99*, 10825–10830.

Kobayashi, D.T., and Chen, K.S. (2005). Behavioral phenotypes of amyloid-based genetically modified mouse models of Alzheimer's disease. Genes Brain Behav. *4*, 173–196.

Lanz, T.A., Hosley, J.D., Adams, W.J., and Merchant, K.M. (2004). Studies of Abeta pharmacodynamics in the brain, cerebrospinal fluid, and plasma in young (plaque-free) Tg2576 mice using the gamma-secretase inhibitor N2-[(2S)-2-(3,5-difluorophenyl)-2-hydroxyethanoyl]-N1-[(7S)-5-methyl-6-oxo-6,7-dihydro-5H-dibenzo[b,d]azepin-7-yl]-L-alaninamide (LY-411575). J. Pharmacol. Exp. Ther. *309*, 49–55.

Lazarov, O., Lee, M., Peterson, D.A., and Sisodia, S.S. (2002). Evidence that synaptically released beta-amyloid accumulates as extracellular deposits in the hippocampus of transgenic mice. J. Neurosci. *22*, 9785–9793.

Liang, W.S., Dunckley, T., Beach, T.G., Grover, A., Mastroeni, D., Walker, D.G., Caselli, R.J., Kukull, W.A., McKeel, D., Morris, J.C., et al. (2007). Gene expression profiles in anatomically and functionally distinct regions of the normal aged human brain. Physiol. Genomics *28*, 311–322.

Liang, W.S., Dunckley, T., Beach, T.G., Grover, A., Mastroeni, D., Ramsey, K., Caselli, R.J., Kukull, W.A., McKeel, D., Morris, J.C., et al. (2008). Altered neuronal gene expression in brain regions differentially affected by Alzheimer's disease: a reference data set. Physiol. Genomics *33*, 240–256.

López-Toledano, M.A., and Shelanski, M.L. (2007). Increased neurogenesis in young transgenic mice overexpressing human APP(Sw, Ind). J. Alzheimers Dis. *12*, 229–240.

Masdeu, J.C., Zubieta, J.L., and Arbizu, J. (2005). Neuroimaging as a marker of the onset and progression of Alzheimer's disease. J. Neurol. Sci. *236*, 55–64.

McDonald, A.J. (1998). Cortical pathways to the mammalian amygdala. Prog. Neurobiol. *55*, 257–332.

Minkeviciene, R., Rheims, S., Dobszay, M.B., Zilberter, M., Hartikainen, J., Fülöp, L., Penke, B., Zilberter, Y., Harkany, T., Pitkänen, A., and Tanila, H. (2009). Amyloid beta-induced neuronal hyperexcitability triggers progressive epilepsy. J. Neurosci. *29*, 3453–3462.

Molinari, S., Battini, R., Ferrari, S., Pozzi, L., Killcross, A.S., Robbins, T.W., Jouvenceau, A., Billard, J.-M., Dutar, P., Lamour, Y., et al. (1996). Deficits in memory and hippocampal long-term potentiation in mice with reduced calbindin D_{28K} expression. Proc. Natl. Acad. Sci. USA *93*, 8028–8033.

Mucke, L., Masliah, E., Yu, G.-Q., Mallory, M., Rockenstein, E.M., Tatsuno, G., Hu, K., Kholodenko, D., Johnson-Wood, K., and McConlogue, L. (2000). High-level neuronal expression of abeta 1-42 in wild-type human amyloid protein precursor transgenic mice: synaptotoxicity without plaque formation. J. Neurosci. *20*, 4050–4058.

Nagahara, A.H., Merrill, D.A., Coppola, G., Tsukada, S., Schroeder, B.E., Shaked, G.M., Wang, L., Blesch, A., Kim, A., Conner, J.M., et al. (2009). Neuroprotective effects of brain-derived neurotrophic factor in rodent and primate models of Alzheimer's disease. Nat. Med. *15*, 331–337.

Nikolaev, A., McLaughlin, T., O'Leary, D.D., and Tessier-Lavigne, M. (2009). APP binds DR6 to trigger axon pruning and neuron death via distinct caspases. Nature *457*, 981–989.

Ognibene, E., Middei, S., Daniele, S., Adriani, W., Ghirardi, O., Caprioli, A., and Laviola, G. (2005). Aspects of spatial memory and behavioral disinhibition in Tg2576 transgenic mice as a model of Alzheimer's disease. Behav. Brain Res. *156*, 225–232.

Palop, J.J., and Mucke, L. (2010). Amyloid-beta-induced neuronal dysfunction in Alzheimer's disease: from synapses toward neural networks. Nat. Neurosci. *13*, 812–818.

Palop, J.J., Jones, B., Kekonius, L., Chin, J., Yu, G.-Q., Raber, J., Masliah, E., and Mucke, L. (2003). Neuronal depletion of calcium-dependent proteins in the dentate gyrus is tightly linked to Alzheimer's disease-related cognitive deficits. Proc. Natl. Acad. Sci. USA *100*, 9572–9577.

Palop, J.J., Chin, J., Roberson, E.D., Wang, J., Thwin, M.T., Bien-Ly, N., Yoo, J., Ho, K.O., Yu, G.-Q., Kreitzer, A., et al. (2007). Aberrant excitatory neuronal activity and compensatory remodeling of inhibitory hippocampal circuits in mouse models of Alzheimer's disease. Neuron *55*, 697–711.

Ramirez, J.J., Campbell, D., Poulton, W., Barton, C., Swails, J., Geghman, K., Courchesne, S.L., and Wentworth, S. (2007). Bilateral entorhinal cortex lesions impair acquisition of delayed spatial alternation in rats. Neurobiol. Learn. Mem. *87*, 264–268.

Remondes, M., and Schuman, E.M. (2004). Role for a cortical input to hippocampal area CA1 in the consolidation of a long-term memory. Nature *431*, 699–703.

Roberson, E.D., Scearce-Levie, K., Palop, J.J., Yan, F., Cheng, I.H., Wu, T., Gerstein, H., Yu, G.-Q., and Mucke, L. (2007). Reducing endogenous tau ameliorates amyloid beta-induced deficits in an Alzheimer's disease mouse model. Science *316*, 750–754.

Roberts, G.W., Nash, M., Ince, P.G., Royston, M.C., and Gentleman, S.M. (1993). On the origin of Alzheimer's disease: a hypothesis. Neuroreport *4*, 7–9.

Scheff, S.W., and Price, D.A. (2003). Synaptic pathology in Alzheimer's disease: a review of ultrastructural studies. Neurobiol. Aging *24*, 1029–1046.

Seeley, W.W., Crawford, R.K., Zhou, J., Miller, B.L., and Greicius, M.D. (2009). Neurodegenerative diseases target large-scale human brain networks. Neuron *62*, 42–52.

Selkoe, D.J. (2008). Soluble oligomers of the amyloid beta-protein impair synaptic plasticity and behavior. Behav. Brain Res. *192*, 106–113.

Shankar, G.M., Li, S., Mehta, T.H., Garcia-Munoz, A., Shepardson, N.E., Smith, I., Brett, F.M., Farrell, M.A., Rowan, M.J., Lemere, C.A., et al. (2008). Amyloid-beta protein dimers isolated directly from Alzheimer's brains impair synaptic plasticity and memory. Nat. Med. *14*, 837–842.

Sheng, J.G., Price, D.L., and Koliatsos, V.E. (2002). Disruption of corticocortical connections ameliorates amyloid burden in terminal fields in a transgenic model of Abeta amyloidosis. J. Neurosci. *22*, 9794–9799.

Spencer, B., Rockenstein, E., Crews, L., Marr, R., and Masliah, E. (2007). Novel strategies for Alzheimer's disease treatment. Expert Opin. Biol. Ther. *7*, 1853–1867.

Sperling, R.A., Laviolette, P.S., O'Keefe, K., O'Brien, J., Rentz, D.M., Pihlajamaki, M., Marshall, G., Hyman, B.T., Selkoe, D.J., Hedden, T., et al. (2009). Amyloid deposition is associated with impaired default network function in older persons without dementia. Neuron *63*, 178–188.

Squire, L.R., Stark, C.E., and Clark, R.E. (2004). The medial temporal lobe. Annu. Rev. Neurosci. *27*, 279–306.

Steffenach, H.A., Witter, M., Moser, M.B., and Moser, E.I. (2005). Spatial memory in the rat requires the dorsolateral band of the entorhinal cortex. Neuron *45*, 301–313.

Sun, B., Zhou, Y., Halabisky, B., Lo, I., Cho, S.H., Mueller-Steiner, S., Devidze, N., Wang, X., Grubb, A., and Gan, L. (2008). Cystatin C-cathepsin B axis regulates amyloid beta levels and associated neuronal deficits in an animal model of Alzheimer's disease. Neuron *60*, 247–257.

Sun, B., Halabisky, B., Zhou, Y., Palop, J.J., Yu, G.Q., Mucke, L., and Gan, L. (2009). Imbalance between GABAergic and glutamatergic transmissions impairs adult neurogenesis in an animal model of Alzheimer's disease. Cell Stem Cell *5*, 624–633.

Sze, C.I., Troncoso, J.C., Kawas, C., Mouton, P., Price, D.L., and Martin, L.J. (1997). Loss of the presynaptic vesicle protein synaptophysin in hippocampus correlates with cognitive decline in Alzheimer disease. J. Neuropathol. Exp. Neurol. *56*, 933–944.

Tanzi, R.E. (2005). The synaptic Abeta hypothesis of Alzheimer disease. Nat. Neurosci. *8*, 977–979.

Tanzi, R.E., and Bertram, L. (2005). Twenty years of the Alzheimer's disease amyloid hypothesis: a genetic perspective. Cell *120*, 545–555.

Terry, R.D., Masliah, E., Salmon, D.P., Butters, N., DeTeresa, R., Hill, R., Hansen, L.A., and Katzman, R. (1991). Physical basis of cognitive alterations in Alzheimer's disease: synapse loss is the major correlate of cognitive impairment. Ann. Neurol. *30*, 572–580.

Tomiyama, T., Matsuyama, S., Iso, H., Umeda, T., Takuma, H., Ohnishi, K., Ishibashi, K., Teraoka, R., Sakama, N., Yamashita, T., et al. (2010). A mouse model of amyloid beta oligomers: their contribution to synaptic alteration, abnormal tau phosphorylation, glial activation, and neuronal loss in vivo. J. Neurosci. *30*, 4845–4856.

Tuszynski, M.H., Thal, L., Pay, M., Salmon, D.P., U, H.S., Bakay, R., Patel, P., Blesch, A., Vahlsing, H.L., Ho, G., et al. (2005). A phase 1 clinical trial of nerve growth factor gene therapy for Alzheimer disease. Nat. Med. *11*, 551–555.

Van Groen, T., and Wyss, J.M. (2003). Connections of the retrosplenial granular b cortex in the rat. J. Comp. Neurol. *463*, 249–263.

van Groen, T., Miettinen, P., and Kadish, I. (2003). The entorhinal cortex of the mouse: organization of the projection to the hippocampal formation. Hippocampus *13*, 133–149.

van Strien, N.M., Cappaert, N.L., and Witter, M.P. (2009). The anatomy of memory: an interactive overview of the parahippocampal-hippocampal network. Nat. Rev. Neurosci. *10*, 272–282.

Vann, S.D., Aggleton, J.P., and Maguire, E.A. (2009). What does the retrosplenial cortex do? Nat. Rev. Neurosci. *10*, 792–802.

Walsh, D.M., and Selkoe, D.J. (2004). Deciphering the molecular basis of memory failure in Alzheimer's disease. Neuron *44*, 181–193.

Wei, W., Nguyen, L.N., Kessels, H.W., Hagiwara, H., Sisodia, S., and Malinow, R. (2010). Amyloid beta from axons and dendrites reduces local spine number and plasticity. Nat. Neurosci. *13*, 190–196.

Weidemann, A., Paliga, K., Dürrwang, U., Reinhard, F.B.M., Schuckert, O., Evin, G., and Masters, C.L. (1999). Proteolytic processing of the Alzheimer's disease amyloid precursor protein within its cytoplasmic domain by caspase-like proteases. J. Biol. Chem. *274*, 5823–5829.

Wu, W., and Small, S.A. (2006). Imaging the earliest stages of Alzheimer's disease. Curr. Alzheimer Res. *3*, 529–539.

Wyss, J.M., and Van Groen, T. (1992). Connections between the retrosplenial cortex and the hippocampal formation in the rat: a review. Hippocampus *2*, 1–11.

Yasuda, M., and Mayford, M.R. (2006). CaMKII activation in the entorhinal cortex disrupts previously encoded spatial memory. Neuron *50*, 309–318.